Residual Strength Analysis Methodology: Laboratory Coupons to Structural Components

D. S. Dawicke, J. C. Newman, Jr., J. H. Starnes, Jr., C. A. Rose, R. D. Young
NASA Langley Research Center

and

B. R. Seshadri
National Research Council

Abstract

The NASA Aircraft Structural Integrity (NASIP) and Airframe Airworthiness Assurance/Aging Aircraft (AAA/AA) Programs have developed a residual strength prediction methodology for aircraft fuselage structures. This methodology has been experimentally verified for structures ranging from laboratory coupons up to full-scale structural components. The methodology uses the critical crack tip opening angle (CTOA) fracture criterion to characterize the fracture behavior and a material and a geometric nonlinear finite element shell analysis code to perform the structural analyses.

The present paper presents the results of a study to evaluate the fracture behavior of 2024-T3 aluminum alloys with thickness of 0.04 inches to 0.09 inches. The critical CTOA and the corresponding plane strain core height necessary to simulate through-the-thickness effects at the crack tip in an otherwise plane stress analysis, were determined from small laboratory specimens. Using these parameters, the CTOA fracture criterion was used to predict the behavior of middle crack tension specimens that were up to 40 inches wide, flat panels with riveted stiffeners and multiple-site damage cracks, 18-inch-diameter pressurized cylinders, and full scale curved stiffened panels subjected to internal pressure and mechanical loads.

Introduction

The ability to predict analytically the residual strength of aircraft fuselage structures requires methodologies that account for both material and geometric nonlinearities. Thin, ductile fuselage skin materials typically exhibit large-scale yielding and significant amounts of stable crack growth, limiting the applicability of linear elastic fracture mechanics (LEFM) based techniques. The presence of cracks in a fuselage structure can result in large (relative to the skin thickness) out-of-plane displacements that are coupled with internal loads. This coupling can magnify the magnitudes of the crack tip stresses and displacements beyond that predicted from linear structural analyses.

The NASA Aircraft Structural Integrity and Airframe Airworthiness Assurance Programs [1] have examined residual strength prediction methodologies based on elastic-plastic fracture mechanics (EPFM) and geometrically nonlinear structural analyses. The critical crack tip opening angle (CTOA) fracture criterion [2-4] was used to predict the stable tearing behavior of the fuselage skin 2024-T3 aluminum alloy. This criterion assumes that stable crack growth will occur when the local crack opening angle displacement

reaches a critical value and requires an elastic-plastic finite element analysis to implement the criterion. The three-dimensional (geometrically linear) finite element code ZIP3D [5] was used to perform residual strength predictions for simple laboratory specimens that did not exhibit (or were prevented from exhibiting) large out-of-plane displacements. The nonlinear shell analysis code STAGS [6], was used to perform the residual strength analyses for the specimens and structures that experienced geometric nonlinearities.

An extensive experimental program was conducted to verify these methodologies based on a test plan that started with simple laboratory specimens and progressed to more complex and more structurally realistic stiffened panel specimens. Small laboratory coupon specimens were tested to characterize the fracture behavior of the 2024-T3 alloy for several thicknesses. Larger specimens and specimens of different configurations were tested to verify that the EPFM fracture parameters obtained from the small specimens could predict the fracture behavior of the larger specimens. The ability of the methodologies to predict geometric nonlinear responses was verified by comparison of the numerical results with out-of-plane displacement measurements made during tests of wide, thin sheets with long, narrow center notches. The compressive stresses parallel to the direction of the notches resulted in local sheet buckling, with measured out-of-plane displacements as great as 20 times the thickness (generally, out-of-plane displacements greater than half of the thickness is considered to be a geometrically nonlinear condition for thin shells). Large, thin sheets with multiple cracks and riveted stiffeners were fractured to represent more of the structural details, yet maintain simple boundary conditions. These specimen required the modeling of crack interaction effects, crack-stiffener effects, and crack buckling. Cracked, pressurized cylinders were tested to simulate the fracture of a pressurized fuselage with simple boundary conditions and without complex structural details. The final step in the experimental evaluation was the testing of a full sized fuselage panel that was loaded with internal pressure plus axial tension loads. The panel was designed to represent a generic wide body commercial transport aircraft and had multiple cracks.

The objectives of the present paper is to describe the CTOA fracture criterion and the geometrically nonlinear structural analysis, and the use these methodologies to predict residual strength of aircraft fuselage structures. Predictions will be made for a wide range of experimental configurations, from very simple laboratory specimens to complex fuselage panels. The material used in the experiments was 2024-T3 aluminum alloy in thicknesses of 0.04, 0.063, and 0.09 inches. In all cases, the fracture parameters used in the residual strength predictions were obtained from the small laboratory specimens and were used to predict the behavior of the more complex configurations. With the exception of the fuselage panel tests and the corresponding small specimen tests conducted for material characterization, all of the specimens were orientated in the L-T direction (crack perpendicular to the rolling direction). The material in the fuselage panel tests was orientated with the T-L orientation (crack parallel to the rolling direction). Unless specifically noted, all of the reported experimental measurements and analysis results are for the material in the L-T orientation.

Analysis Methodology

The fracture behavior of thin, ductile aluminum alloys is characterized by large scale yielding at the crack tip and large amounts of stable tearing prior to reaching the critical load. The use of linear elastic fracture mechanics (LEFM) based parameters, like a stress-intensity factor (K), cannot predict "scaling" effects. In other words, a linear elastic parameter can predict the behavior of specimens with similar sizes, but cannot predict the behavior of larger or smaller specimens. Elastic-plastic approximations have been incorporated into LEFM parameters using a plasticity correction factor and a resistance curve approach. A resistance curve assumes that the stable tearing process is characterized by a unique relationship between the fracture parameter and the extent of stable crack growth. Thus, the fracture behavior for any configuration can be determined if the resistance curve for a material is known. The characterization of the resistance curve requires large amounts of stable tearing and can only be obtained from large specimen fracture tests. Thus, it is possible to predict the behavior of smaller configurations from large panel tests, but predictions of structures larger than that for which the resistance curved was obtained, would require extrapolation. To predict the behavior of large structures from material behavior obtained from small laboratory coupon specimens requires a fracture criterion that is independent of the amount of stable crack growth.

The critical crack tip opening angle (CTOA) fracture criterion is an elastic-plastic fracture criterion that is independent of stable crack growth and requires an elastic-plastic finite element analysis for implementation. Cracks in a pressurized fuselage structure can result in large out-of-plane displacements that are coupled with internal stresses. A geometrically nonlinear finite element analysis is required to model accurately this behavior. The following sections describe the CTOA fracture criterion, how it is incorporated into a finite element analysis, and how the CTOA criterion can be implemented in a geometrically nonlinear finite element analysis to predict fracture behavior with local crack buckling or bulging.

CTOA Fracture Criterion

The CTOA fracture criterion assumes that the crack growth will occur when the angle made by the upper crack surface, the crack tip, and the lower crack surface reaches a critical value, as illustrated in Figure 1. For the 2024-T3 aluminum alloy, a fixed distance of 0.04 inches was used to evaluate the CTOA value [7, 8]. The critical CTOA value can be obtained experimentally using a photographic techniques [8], but significant scatter is usually present in the measurements, as seen in Figure 2. A better method [7] of obtaining the critical value is to simulate the fracture behavior of a laboratory specimen and determine the angle that best describes the fracture behavior. To predict the fracture behavior of other configurations requires a three-dimensional, elastic-plastic finite element analysis that evaluates the CTOA along the mid-plane at a distance 0.04 inches behind the crack tip and allows the crack to advance when the critical value is achieved.

The 0.04 inch-long distance behind the crack is defined relatively arbitrarily. As this distance decreases, the size of the crack tip elements in the finite element analysis must also decrease. Too large of a distance will result in a lack of sensitivity to the behavior at the crack tip. Also, the value of the critical CTOA is influenced by the distance behind

the crack tip. For a given material, the critical CTOA will decrease as the distance behind the crack tip increases. The distance also specifies the amount of crack extension that is released in the finite element analysis when the critical CTOA is achieved. Three considerations are important in the selection of the distance: (1) the same value is used for all analyses of a given material; (2) the distance should be less than 20% of the total crack extension, prior to achieving maximum load, in the experiments used to determine the critical CTOA; and (3) the distance must allow convergence of crack opening displacements that are obtained in the finite element analyses.

Implementation of CTOA in a Finite Element Analysis

The CTOA fracture criterion can be easily implemented into an elastic-plastic finite element analysis. In a two-dimensional analysis, the displacements δ, perpendicular to the crack, at a fixed distance d behind the crack tip (defined as d = 0.04 inches in the present paper) are monitored during the analytical loading of the model. When the displacements are such that the critical angle (ψ_c) is attained (equation 1), the crack is advanced by releasing the crack tip nodes until a total of 0.04 inches of crack growth is achieved. Then, the applied displacements are held constant while the internal forces are returned to equilibrium.

$$\psi_c = 2\tan^{-1}\left(\frac{\delta}{d}\right) \qquad (1)$$

A two-dimensional analysis must be either plane stress or plane strain. However, the local state of stress at the crack tip is neither plane stress nor plane strain, but rather something in between [7]. This condition requires an approximation to describe the actual state of stress. The plane strain core approximation assumes that a thin strip of elements, of height h_c, is defined as having plane strain conditions, while the remainder of the model has plane stress conditions, as illustrated in Figure 3.

The implementation of the CTOA criterion in a three-dimensional model is identical to the two-dimensional model implementation, except that the displacements are monitored along the mid-thickness at a distance of 0.04 inches behind the crack. When the displacements are such that the critical angle is obtained, the crack is advanced by releasing the crack tip nodes until a total of 0.04 inches of crack growth is achieved along the entire crack front. This approach neglects the effect of crack tunneling. To approximate crack tunneling effects, the displacements at all the nodes along the crack front, at a distance of 0.04 inches behind the crack tip, could be evaluated and crack advance allowed only at locations through-the-thickness where the critical CTOA has been achieved. The modeling of tunneling would require a more refined mesh in the crack plane.

A convergence study is required for each finite element mesh in a CTOA analysis. Convergence of the displacements at the CTOA measurement location is necessary for the fracture criterion to predict accurately the behavior of structures of different sizes and configurations. Convergence has been obtained using the following crack plane element sizes and a CTOA evaluation distance of d = 0.04 inches:

Two-dimensional models

- constant strain triangular elements - 0.02 inches long by 0.02 inches high
- quadratic, quadrilateral elements - 0.04 inches long by 0.04 inches high

Three-dimensional models

- linear, 8-node elements - 0.04 inches long by 0.04 inches high by a quarter of the thickness (for thickness less than 0.09 inches)

These guidelines should be used as a starting point for a convergence study. Actual convergence will be influenced by the amount of crack extension prior to reaching the maximum load, the thickness of the material, and the presence of local crack buckling. Small structures that have critical crack lengths less than 5d will require smaller elements than listed above and the analysis will typically overpredict the critical stress. Structures that are thicker than 0.1 inches may require more than 2 elements through the half-thickness. A structure that experiences out-of-plane buckling may require smaller elements not only around the crack plane, but also in the region of large out-of-plane displacement gradients.

Geometrically Nonlinear Structural Analysis

A large, cracked, thin structure will experience large out-of-plane displacements, i.e. it bends or it buckles. A geometrically nonlinear analysis is required to describe accurately the magnified crack tip stresses resulting from the coupling of the out-of-plane displacements and the internal stresses. To initiate the buckling response, an initial out-of-plane imperfection is incorporated into the finite element mesh. The imperfection takes the form of the lowest eigenvector of the buckling solution with a magnitude of 1% of the thickness. The CTOA fracture criterion was implemented into the geometrically nonlinear analysis in the same manner described in the previous section for a geometrically linear analysis.

Predictions and Experimental Verification

Fracture predictions were made on three thicknesses of 2024-T3 aluminum alloy. For each thickness, the critical CTOA was obtained by simulating the fracture behavior of 6-inch-wide compact tension specimens. The critical CTOA values were then used to predict the behavior of fracture tests conducted on specimens ranging from small laboratory coupons to a full-size fuselage panel. The ZIP3D [5] finite element code was used to determine the critical CTOA and to predict the behavior of the non-buckled specimens. The STAGS [6] geometrically nonlinear analysis code, using the plane strain core approximation, was used to predict the behavior of the tests with large out-of-plane displacements.

CTOA Determination

The critical CTOA for the 2024-T3 aluminum alloy was determined by simulating the fracture behavior of 6-inch-wide compact tension, C(T), specimens with thicknesses of B = 0.04, 0.063, and 0.09 inches. All specimens had the same initial crack length to width ratio a/W = 0.4 and the same fatigue precrack stress-intensity factor range and stress ratio (ΔK = 7 ksi inch$^{1/2}$, R = 0.1). The analyses were conducted using the ZIP3D finite element code. The only difference in material properties between the three thicknesses was the stress-strain curve. A piece-wise linear curve was used for each of the three thicknesses, as summarized in Table 1. The finite element meshes were identical for each simulation, with crack plane element dimensions in the x- (crack length), y- (loading), and z-directions (through-thickness), of 0.04 inch, 0.04 inch, and B/4 respectively.

The test measurements and the simulated load versus crack extension values are shown in Figure 4. The simulations and tests agreed well for the 0.09 inch and 0.04 inch thick tests, describing both the magnitude and shape of the experimental measurements. The simulation for the 0.063-inch-thick specimens had the shape of the experimental measurements, but the maximum load was about 5% less than the measured value. The resultant critical angle decreased almost linearly with increasing thickness, as shown in Figure 5.

Non-Buckled Coupon Tests

Fracture tests were conducted with several sizes of compact tension, C(T), and middle crack tension, M(T), specimens. The width of the C(T) specimens were 2 < W < 6 inches and the width of the M(T) specimens were 3 < W < 40 inches. Guide plates were used prevent out-of-plane displacements in both the C(T) and M(T) specimens. The C(T) guide plates consisted of two 1/4-inch-thick steel plates that "sandwiched" the specimen. The M(T) guide plates consisted of four 1/2-inch-thick plates that "sandwiched" the specimen, both above and below the crack plane, as shown in Figure 6. The top and bottom "sandwiches" were separated to prevent load transfer through the guide plates. A thin layer of Teflon was placed between the specimen and the plates to allow the specimen to slide between the plates. The guide plates for the 40-inch-wide M(T) specimens were augmented with six sets of 3-inch-deep steel I-beams to further restrict the out-of-plane displacements. These I-beams were added because the large, thin specimens experienced severe buckling that deformed the 1/2-inch-thick plates.

The critical CTOA values used in the ZIP3D finite element analyses were determined from the 6-inch-wide, C(T) fracture tests: 5.25^o for B = 0.09 inch, 5.4^o for B = 0.063 inch, and 5.6^o for B = 0.04 inch. The maximum loads obtained during each C(T) fracture test are shown in Figure 7. Tests were conducted on 2-, 4-, and 6-inch-wide C(T) specimens for the B = 0.09 inch and B = 0.063 inch aluminum alloys, but only on 6-inch-wide wide C(T) specimens for the B = 0.04 inch thick material. The elastic-plastic finite element analyses with the CTOA fracture criterion predicted the maximum load to within 5% of the experimental measurements.

The maximum stresses obtained during the M(T) fracture tests are shown in Figure 8. Tests were conducted on 1.2-, 3-, 12-, and 24-inch-wide specimens for the B = 0.09 inch; 3-, 12-, 24-, and 40-inch-wide specimens for the B = 0.063 inch; and 12-inch wide specimens for the B = 0.04 inch thick aluminum alloys. The critical CTOA values used in the analyses were determined from the 6-inch-wide, C(T) fracture tests: 5.25^o for B = 0.09 inch; 5.4^o for B = 0.063 inch; and 5.6^o for B = 0.04 inch. The elastic-plastic finite element analyses with the CTOA fracture criterion predicted the maximum stress to within 5% of the experimental measurements.

Additional tests were conducted to examine the effect of crack length and crack interaction effects due to multiple site damage (MSD). To examine crack length effects, tests were conducted on 12-inch-wide, 0.09-inch-thick M(T) specimens with different initial crack lengths. The critical CTOA value of 5.25^o was used to predict the fracture behavior, as shown in Figure 9. The CTOA fracture analysis accurately predicted both the magnitude of the maximum stress and the crack extension behavior for all three initial crack lengths.

The presence of MSD can significantly influence the residual strength of a structure. The fracture behavior of two tests conducted on a 0.09-inch-thick, 12-inch-wide 2024-T3 aluminum alloy specimen is represented in Figure 10. Both tests had a 4-inch-=long center crack, but the MSD test also had a 0.5-inch-long crack near each tip of the lead crack, as shown in Figure 10. The cracks in both specimens started to grow at about the same applied stress level, but in the MSD specimen, the center crack and lead cracks linked-up and failed at a significantly lower load then observed in the single crack test. The ZIP3D finite element code with the CTOA fracture criterion (critical value of 5.25^o) was used to predict the behavior of both tests. The finite element analyses predicted the stress at link-up and failure in the MSD test to within 3% of the experimental measurements.

A series of fracture tests with specimens with two and three cracks were conducted to further examine the ability of the CTOA fracture criterion to predict the fracture behavior of MSD conditions. The 2-crack test series consisted of a 12-inch-wide, 0.09-inch-thick sheet of 2024-T3 aluminum alloy with two 2-inch-long cracks. Three tests were conducted with different ligament lengths b between the two cracks, as shown in Figure 11. The stress at link-up and the maximum stress were recorded for each test. The ZIP3D finite element code with the CTOA fracture criterion (critical value of 5.25^o) was

used to predict the behavior of specimens tests and was able to predict the link-up stresses and maximum stresses to within 3% of the experimental measurements.

A similar study was performed on a 3-crack configuration that consisted of a 4-inch-long center crack and two 0.5-inch-long MSD cracks (each MSD crack was at a distance b from one of the tips of the 4-inch-long crack), as shown in Figure 12. The test specimen was 12-inches wide, 0.09-inches thick, and made of 2024-T3 aluminum alloy, and the critical CTOA value was 5.25^{o}. Again, the link-up stresses and maximum stresses were predicted to within 3% of the experimental measurements.

Fracture tests were conducted on 0.063-inch-thick, 2024-T3 aluminum alloy specimens in the T-L orientation, and results are shown in Figure 13. The tests were conducted on 3-, 12-, and 24-inch-wide M(T) specimens with guide plates to restrict out-of-plane displacements. For 2024-T3, the T-L orientation typically has about a 15% reduction in the residual strength as compared to the L-T orientation. This is reflected in a corresponding reduction in the critical CTOA value. The ZIP3D finite element codes with the CTOA fracture criterion (critical value of 5^{o}) was used to predict the behavior of the tests.

Plane Strain Core

A three-dimensional finite element code requires only the critical CTOA to predict the fracture behavior of thin, aluminum materials because the through-thickness constraint effects are accounted for implicitly in the model. In addition to the critical CTOA, a two-dimensional finite element analysis requires the plane strain core approximation to account for the through-thickness constraint effects. This two-parameter requirement increases the complexity of determining the correct values from a small specimen fracture test. To simplify this process, the critical CTOA is first determined from a three-dimensional analysis. Then, using this CTOA value, two-dimensional analyses are conducted, changing the plane strain core height until the analysis agrees with the experimental measurements. As a "rule of thumb", the plane strain core height should be approximately equal to or less than the specimen thickness.

The C(T) fracture test results shown in Figure 4 were used to obtain the value of the plane strain core height using the STAGS nonlinear shell analysis code. The size of the crack plane elements used in these analyses were 0.04 inch by 0.04 inch, allowing for discrete values of plane strain core height (i.e., 0, 0.04, 0.08, 0.12 inches, …). The experimental fracture test results for the 6-inch-wide 2024-T3 aluminum alloy specimens and the STAGS predictions are shown in Figure 14. The critical CTOA values obtained from the ZIP3D analyses (5.25^{o} for B = 0.09 inch, 5.4^{o} for B = 0.063 inch, and 5.6^{o} for B = 0.04 inch) were used in the STAGS analyses. The resulting plane strain core (PSC) heights that provided the best fit to the experimental measurements were: PSC = 0.08 inch for B = 0.09 inch, PSC = 0.08 inch for B = 0.063 inch, and PSC = 0.04 inch for B = 0.04 inch, as shown in Figure 14. The quantum nature of the available PSC values resulted in the PSC for B = 0.063 inch to be either 0.08 inch or 0.04 inch, while the "best" value should probably be around 0.06 inch, as shown in Figure 15.

The fracture behavior of the 0.063-inch-thick, 2024-T3 aluminum alloy M(T) specimens with the crack orientated in the T-L direction were also examined using the STAGS analysis code. The critical CTOA value of 5^{o}, obtained from the ZIP3D analyses were used in the STAGS analyses. The resulting plane strain core height (PSC) that provided the best fit to the experimental measurements was PSC = 0.04 inches, as shown in Figure 16.

Buckling Panel Tests

The STAGS nonlinear shell analysis code was used to predict the fracture behavior of M(T) specimens conducted with and without guide plates to restrict out-of-plane buckling. The model consisted of plane stress quadrilateral shell elements with a plane strain core. The critical CTOA values and height of the plane strain core vary with material thickness as described in the previous sections. The ratio of initial crack length to specimen width was held constant for each test (2a/W = 1/3).

The failure stress for the 0.09 inch thick aluminum alloy M(T) fracture tests, with and without guide plates are shown in Figure 17. The STAGS analysis slightly over predicted the failure stress for the smaller specimen, but was within 3% of the failure stress for the specimens with widths greater than 12 inches. The analysis may be over predicting the behavior of the smaller specimens due to the small amount of crack extension prior to reaching the failure stress. For the 3-inch-wide specimens, the failure stress was achieved after about 0.15 inches of crack growth, which is less 4 elements of crack growth.

The failure stress for the 0.063-inch-thick aluminum alloy M(T) fracture tests, with and without guide plates are shown in Figure 18. The STAGS predictions were within 3% of the failure stress for the specimens with widths less than 40 inches. The analysis over predicted the behavior of the 40-inch-wide specimens with and without guide plates by about 10%.

The maximum stress for the 0.04-inch-thick aluminum alloy M(T) fracture tests, with and without guide plates are shown in Figure 19. The only experiments conducted were on 12-inch-wide M(T) specimens, with and without guide plates. The STAGS predictions were within 3% of the maximum stress for the test with guide plates, but over predicted the behavior of the test without guide plates by about 8%.

MSD Stiffened Panel Tests

Fracture tests were conducted on 40-inch-wide, 0.063 inch thick sheets of 2024-T3 aluminum alloy specimens [9]. The crack configuration of the specimens consisted of a single 8-inch-long center crack with an array of twelve 3/16-inch-diameter holes on either side of the of the center crack. Three different equal MSD crack arrangements (0.01, 0.03, and 0.05 inches from the edge of the hole) were tested. A total of 10 specimens were tested, five with and five without riveted 7075-T3 aluminum alloy stiffeners. The five stiffeners were 1.6-inches-wide and placed on both sides of the specimen, as illustrated in Figure 20. The specimens were tested without guide plates to allow out-of-plane displacements.

Predictions of the fracture behavior were conducted with the STAGS analysis code, a critical CTOA value of 5.4^{o}, and a plane strain core height of 0.08 inch. The configuration and loading condition were symmetric, so only a quarter of the sheet and stiffeners were modeled. The model contained 13,145 shell elements, 17,287 nodes, and 97,254 degrees-of-freedom. The minimum element size along the line of crack extension was 0.04 inches. The analysis did not explicitly model the holes, but assumed that the holes with MSD cracks could be approximated with a crack with a length equal to the sum of the MSD crack lengths and the hole diameter. The rivet connections between the stiffener and sheet were modeled with nonlinear spring fastener elements with six degrees-of-freedom. A bifurcation analysis was conducted to determine the first buckling mode shape and this shape was introduced as an imperfection (with a magnitude of about 10% of the thickness) to the non-linear analysis. To prevent penetration, contact elements and multi-point constraint conditions were used to allow the sheet and stiffener surfaces to contact or separate during buckling.

The experimental measurements and finite element predictions for stiffened and unstiffened panels with a single center crack and no MSD are shown in Figure 21. The presence of the stiffener increased the failure load by a factor of 2 over that of the unstiffened panel. The STAGS finite element analysis predicted the failure load of the unstiffened panel to within 2% of the experimental measurements. The prediction for the stiffened panel slightly overpredicted the crack extension, but was within 5% of the failure load.

The experimental measurements and finite element predictions for stiffened and unstiffened panels with a single center crack and 0.05-inch-long MSD cracks at each of the 24 rivet holes are shown in Figure 22. Both the stiffened and unstiffened panels reached the failure load at link-up of the lead crack and the first MSD crack. The STAGS finite element analysis predicted the link-up (failure) load to within 2% of the experimental measurements.

Pressurized Cylinder Tests

Cylindrical shells were fabricated from 0.04-inch-thick 2024-T3 aluminum alloy sheet, with the rolling direction orientated circumferentially. The cylinders were 39-inches long and 18 inches in diameter and were created by connecting the ends of the sheet with a 1.5-inch-wide double lap splice with 0.04-inch-thick splice plates and a single row of rivets on each side of the splice. The crack was simulated by a 0.01-inch-wide saw cut at the specimen mid-length, diametrically opposite to the lap-splice. Specimens with initial crack lengths of 2, 3, and 4 inches were loaded by internal pressure until failure occurred [10]. The crack length was recorded using crack wire gages.

The finite element models used to simulate the response of the cracked shells subjected to internal pressure took advantage of the symmetry of the problem and only a quarter of the shell was modeled. Self-similar crack growth (straight cracks) was assumed and element size along the both line of crack extension and the circumferential direction was 0.04 inches. The critical CTOA value used in the fracture analysis was 5.6^{o} and the plane strain core height was 0.04 inches. An initial geometric imperfection in the form of the lowest eigenmode was used in the nonlinear analyses to initiate the out-of-plane displacements.

The experimental measurements and the STAGS finite element predictions for the pressurized cylinder tests with initial crack lengths of 2, 3, and 4 inches are shown in Figure 23. The analyses predicted the maximum pressure to within 4% of the measured values, but tended to overpredict the pressure required to initiate crack growth. The use of saw cuts would generally cause the analysis to underpredict the pressure required to initiate the crack growth, since a saw cut would require higher loads to initiate crack growth than a sharp fatigue crack [11]. One possible explanation for the overprediction of maximum pressure could be that the intense crack-tip deformations may have caused the crack wire gages to register crack growth before the growth actually occurred.

Fuselage Panel Tests

Fracture tests were conducted on stringer- and frame-stiffened aluminum fuselage panels with a longitudinal lead crack and smaller MSD cracks. The specimen had four stringers and three frames, as shown in Figure 24(a). The panel had a 122-inch radius, a length of 72 inches, and an arc width of 63 inches. The skin was 0.063-inch-thick 2024-T3 aluminum alloy with the sheet rolling direction parallel to the stringers. The stringers were 7075-T6 aluminum alloy inverted hat-sections, spaced 14 inches apart. The frames were 7075-T6 Z-section frames, with a spacing of 22 inches. A riveted lap-joint, with three rows of 0.125-inch-diameter countersunk rivets, was placed in the center of the specimen. Additional detail can be found in Reference 12. The crack configuration consisted of a 10-inch-long longitudinal lead crack with MSD cracks along the third row of rivets of the lap-joint. The MSD cracks were introduced prior to the assembly of the panel by making 0.05-inch-long saw cuts along both sides of the countersunk rivet holes. The cracks were orientated in the T-L direction (crack parallel to the rolling direction).

The finite element model had 11,000 elements and 63,500 degrees of freedom. A half-length symmetry model, with the assumed plane of symmetry about the axial direction,

was used in the analysis. The inner and outer skins of the lap-joint were modeled as discrete layered shells connected with fastener elements. The MSD cracks were modeled by introducing small cracks in the outer skin at the rivet holes directly ahead of the lead crack. The finite element model is shown in Figure 24(b).

The experimental measurements and the STAGS predictions for the fuselage panel test are shown in Figure 25. Both the measurements and analysis results indicate that the maximum pressure was achieved at the link-up of the lead crack and the first MSD crack. The predicted pressure was approximately 10% higher than that observed in the experiment.

Summary

Fracture tests were conducted on thin sheet 2024-T3 aluminum alloy test specimens ranging in size from small laboratory coupons to full size, curved stiffened fuselage panels. A material and geometrically nonlinear analysis is required predict the fracture behavior of this thin, ductile material. The material nonlinearity is necessary for the fracture criterion to "scale" for different size specimens. The geometric nonlinearity is necessary to describe the coupling between the out-of-plane displacements and the internal loads that occur. The fracture behavior for the tests were predicted using the critical CTOA fracture criterion and the ZIP3D and STAGS elastic-plastic finite element codes. The ZIP3D geometrically linear code and was used to predict the behavior of specimens that were constrained to prevent out-of-plane displacements. The STAGS, geometrically nonlinear shell analysis code was used to predict the fracture behavior of specimens with and without constraints that prevent out-of-plane displacements.

The fracture behavior was characterized in the analyses using the critical CTOA fracture. This criterion is influenced by the through-thickness constraint of the crack tip, and thus requires a three-dimensional analysis to be evaluated properly. For a two-dimensional analysis (STAGS for example), the through-thickness constraint effects can be approximated using the plane strain core concept. The critical CTOA and plane strain core (PSC) values were obtained from small laboratory specimens and found to be a function of only material thickness. Thus, for a given thickness, a single value of CTOA and PSC were sufficient to predict the behavior of all of the specimens tested within 10% of the experimental measurements.

References

1. Harris, C. E., Newman, J. C., Jr., Piascik, R. S., and Starnes, J. H., Jr., "Analytical Methodology for predicting the Onset of Widespread Fatigue Damage in Fuselage Structure," Journal of Aircraft, Vol. 35, No. 2, 1998, pp. 307-317.
2. Anderson, H., "Finite Element Representation of Stable Crack Growth," Journal of Mechanics and Physics of Solids, Vol. 21, 1973, pp. 337-356.
3. De Koning, A. U., "A Contribution to the Analysis of Quasi Static Crack Growth in Steel Materials," Fracture 77, Proceedings of the 4th International Conference on Fracture, Vol. 3, 1977, pp. 25-31.

4. Dawicke, D. S., "Residual Strength Predictions Using a Crack Tip Opening Angle Criterion," Proceedings of the FAA-NASA Symposium on the Continued Airworthiness of Aircraft Structures," DOT/FAA/AR-92/2, 1997, pp. 555-566.
5. Shivakumar, K. N. and Newman, J. C., Jr., "ZIP3D - An Elastic and Elastic-Plastic Finite-Element Analysis Program for Cracked Bodies," NASA TM-102753, 1990.
6. Brogan, F. A., Rankin, C. C., and Cabiness, H. D., "STAGS User Manual, Version 3.0," Lockheed Martin Missiles and Space Co., Inc., Advanced Technology Center, Report LMMS P032594, 1998.
7. Dawicke, D. S. and Newman, J. C., Jr., "Residual Strength Predictions for Multiple Site Damage Cracking Using a Three-Dimensional Finite Element Analysis and a CTOA Criterion," Fatigue and Fracture Mechanics: 29th Volume, ASTM STP 1332, 1998, pp. 815-829.
8. Dawicke, D. S. and Sutton, M. A., "Crack Tip Opening Angle Measurements and Crack Tunneling Under Stable Tearing in Thin Sheet 2024-T3 Aluminum Alloy," NASA CR-191523, September, 1993.
9. Seshadri, B. R., Newman, J. C., Jr., Dawicke, D. S., and Young, R. D., "Fracture Analysis of the FAA/NASA Wide Stiffened Panels," Proceedings of the FAA-NASA Symposium on the Continued Airworthiness of Aircraft Structures," DOT/FAA/AR-92/2, 1997, pp. 513-524.
10. Starnes, J. H., Jr. and Rose, C. A., "Stable Tearing and Buckling Responses of Unstiffened Aluminum Shells with Long Cracks," Proceedings of the FAA-NASA Symposium on the Continued Airworthiness of Aircraft Structures," DOT/FAA/AR-92/2, 1997, pp. 601-626.
11. Dawicke, D. S., Newman, J. C., Jr., Sutton, M. A., and Amstutz, B. E., "Influence of Crack History on the Stable Tearing Behavior of a Thin-Sheet Material with Multiple Cracks," NASA Conference Publication 3274, FAA/NASA International Symposium on Advanced Structural Integrity Methods for Airframe Durability and Damage Tolerance, Part 1, 1994, pp. 193-212.
12. Young, R. D., Rouse, M, Ambur, D. R., and Starnes, J. H., Jr. "Residual Strength Pressure Tests and Nonlinear Analyses of Stringer- and Frame-Stiffened Aluminum Fuselage Panels with Longitudinal Cracks," Proceedings of the FAA-NASA Symposium on the Continued Airworthiness of Aircraft Structures," DOT/FAA/AR-92/2, 1997, pp. 408-426.

Table 1
Stress-Strain Curves for the 2024-T3 Aluminum Alloy

B = 0.09 inch		B = 0.063 inch		B = 0.04 inch	
Stress (ksi)	Strain	Stress (ksi)	Strain	Stress (ksi)	Strain
50.0	0.00483	52.5	0.00507	52.5	0.00507
56.5	0.015	55.5	0.01	55.5	0.01
62.5	0.04	59.0	0.02	59.0	0.02
68.5	0.1	63.5	0.04	63.5	0.04
71.0	0.16	68.0	0.07	68.0	0.07
71.0	0.2	70.5	0.1	70.5	0.1
		72.0	0.16	72.0	0.16
		72.0	0.2	72.0	0.2

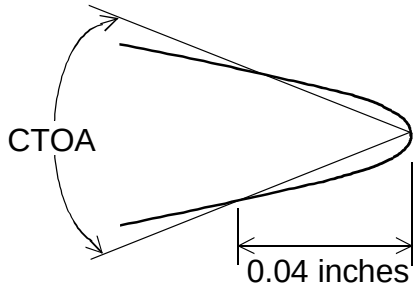

Figure 1 Schematic of the definition of critical crack-tip opening angle (CTOA).

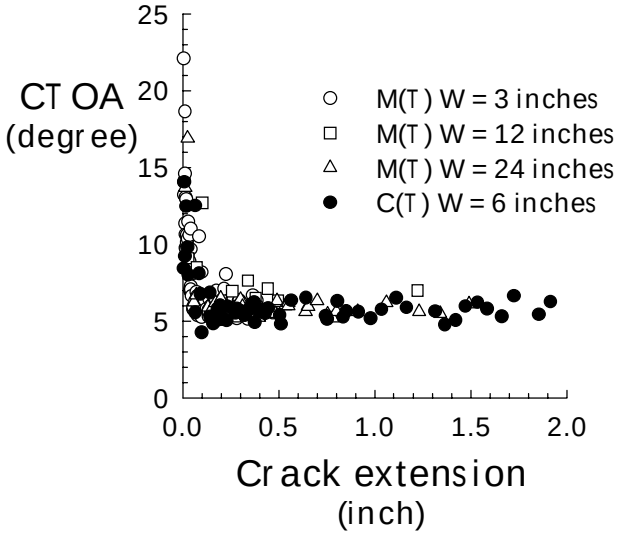

Figure 2 CTOA measurements for 0.063-inch-thick, 2024-T3 aluminum alloy.

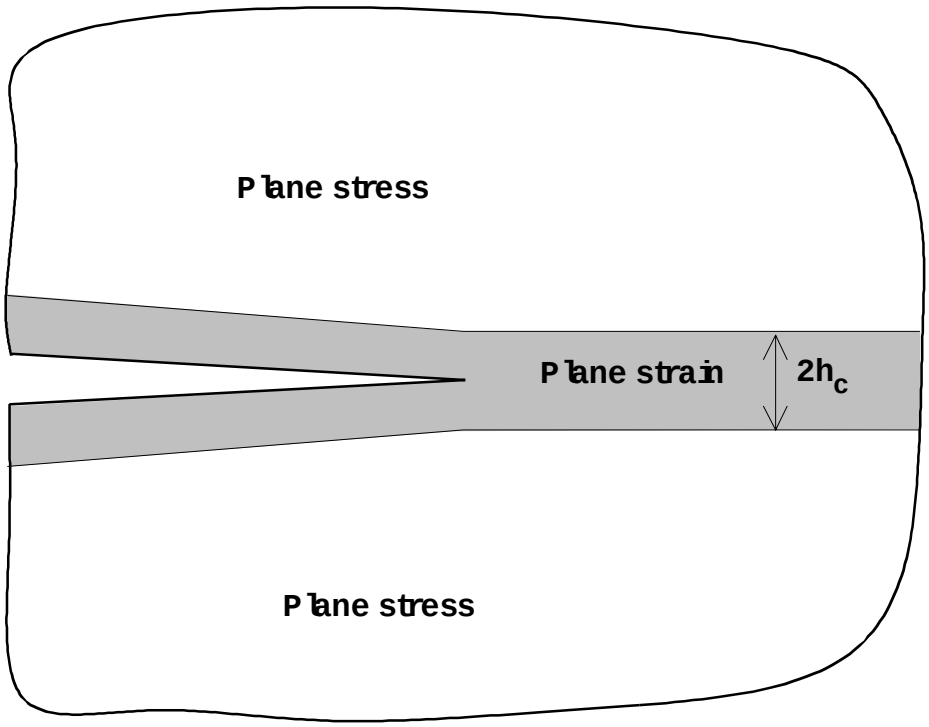

Figure 3 Illustration of the plane strain core around a crack.

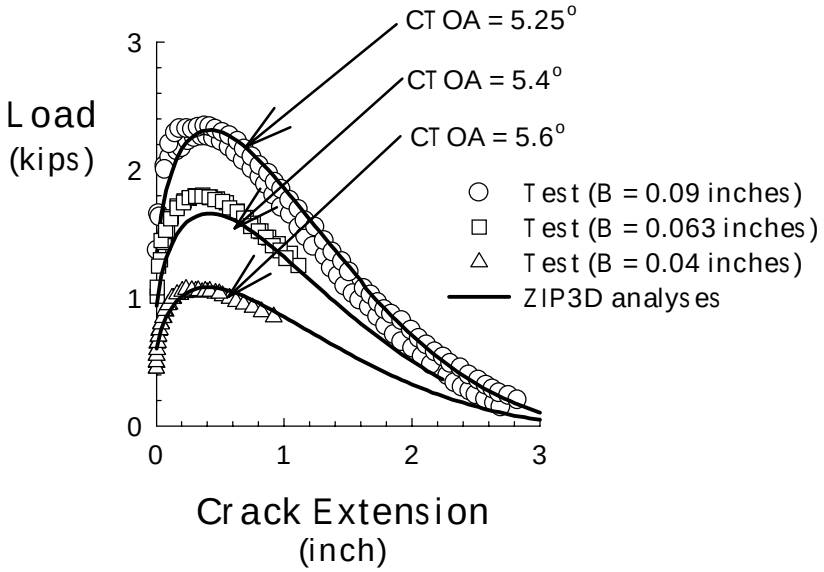

Figure 4 Fracture results from 6-inch-wide C(T) specimens with an initial crack length of a/W = 0.4 and the CTOA simulations using ZIP3D.

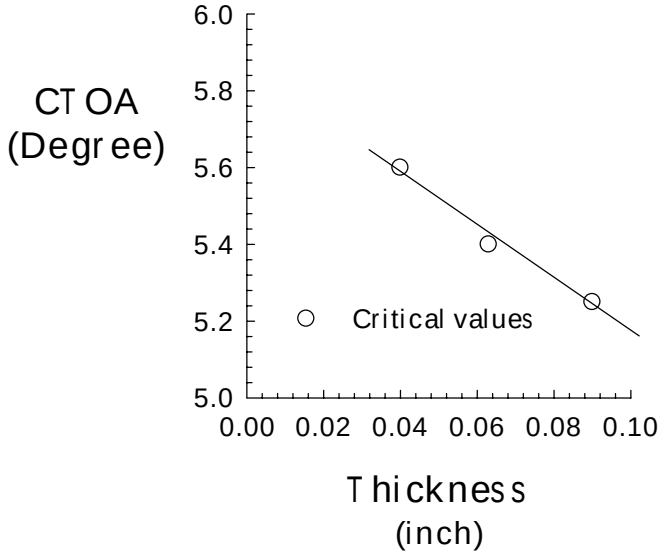

Figure 5 Influence of specimen thickness on the critical CTOA for 2024-T3 aluminum alloy.

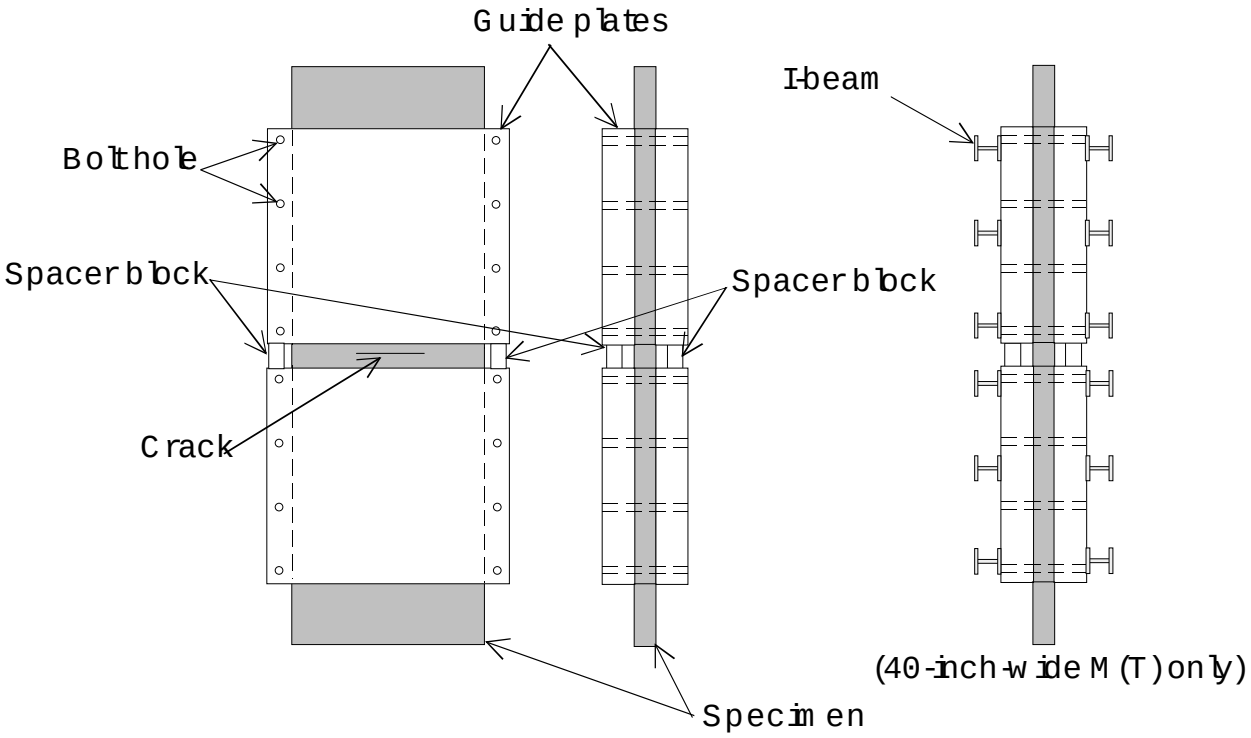

Figure 6 Schematic of M(T) guide plates.

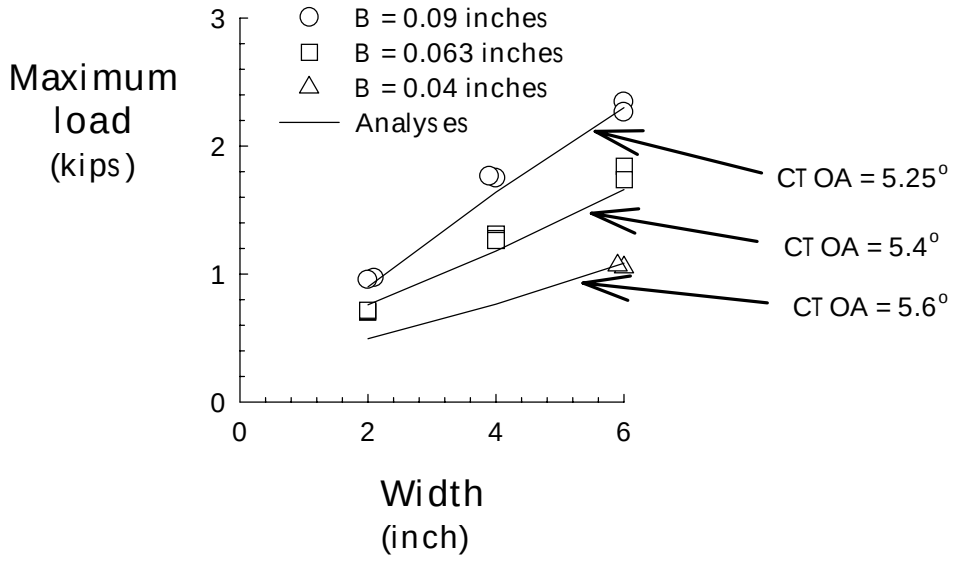

Figure 7 Experimental measurements and the ZIP3D finite element predictions for fracture tests conducted on 2024-T3 aluminum alloy C(T) specimens (initial crack length a/W = 0.4).

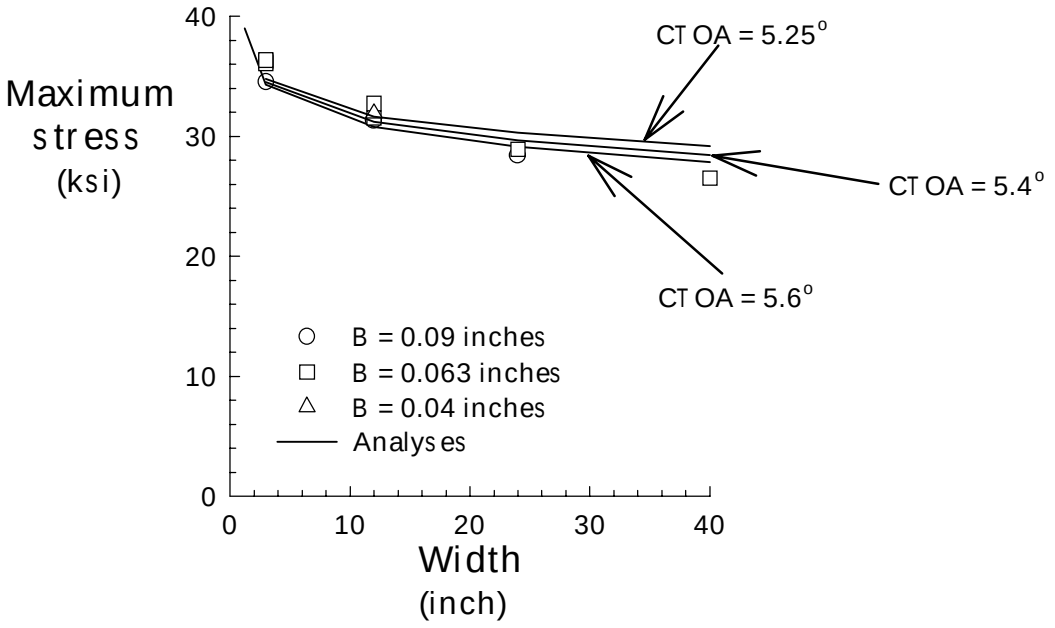

Figure 8 Experimental measurements and the ZIP3D finite element predictions for fracture tests conducted on 2024-T3 aluminum alloy M(T) specimens (initial crack length 2a/W = 1/3)

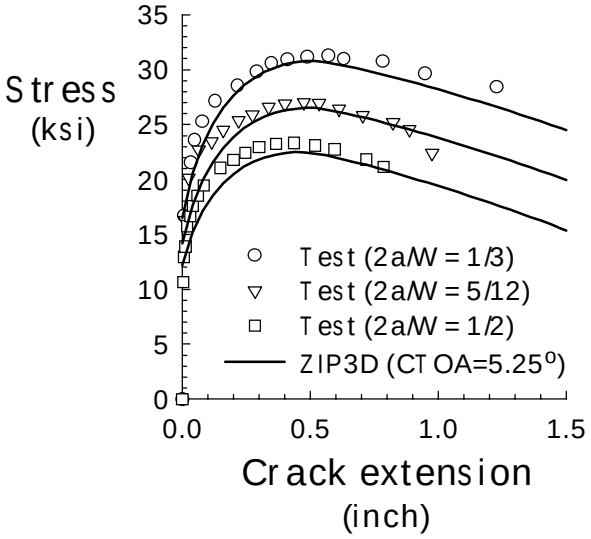

Figure 9 Experimental measurements and the ZIP3D finite element predictions for fracture tests conducted on 2024-T3 aluminum alloy M(T) specimens at different initial crack lengths.

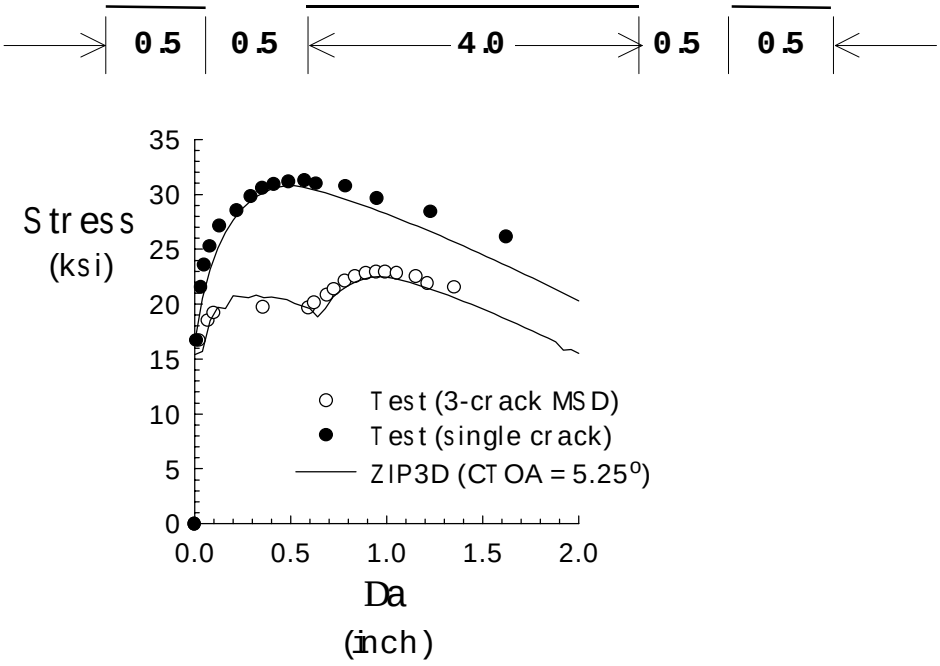

Figure 10 Experimental measurements and the ZIP3D finite element predictions for fracture tests conducted on a 12-inch-wide, 2024-T3 aluminum alloy, 3-crack specimens and an identical specimen with just a single, 4-inch-long crack.

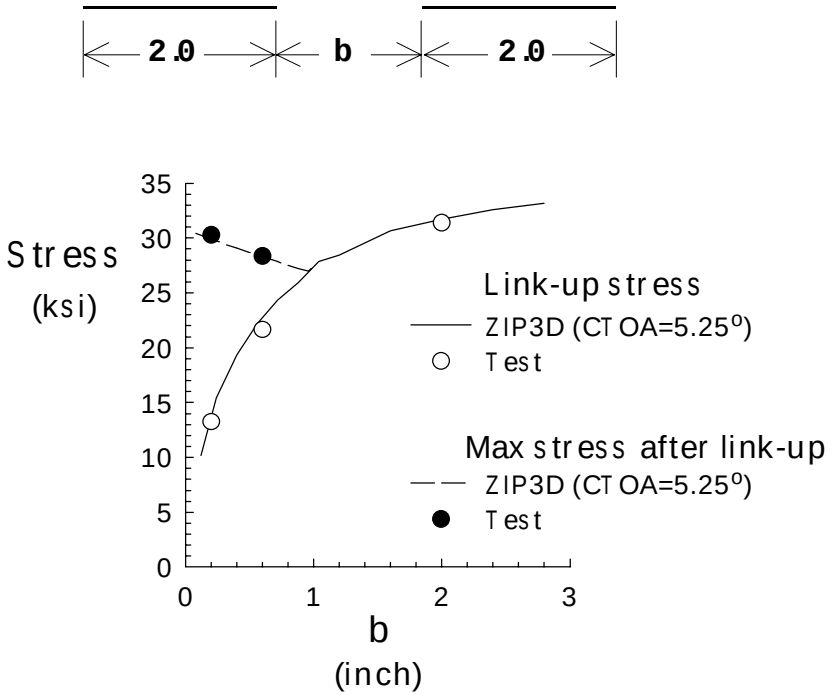

Figure 11 Experimental measurements and finite element predictions for fracture tests conducted on 12-inch-wide, 2024-T3 aluminum alloy, 2-crack specimens.

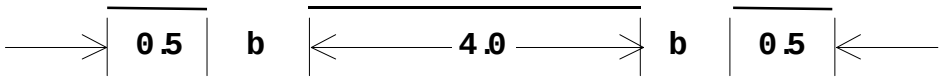

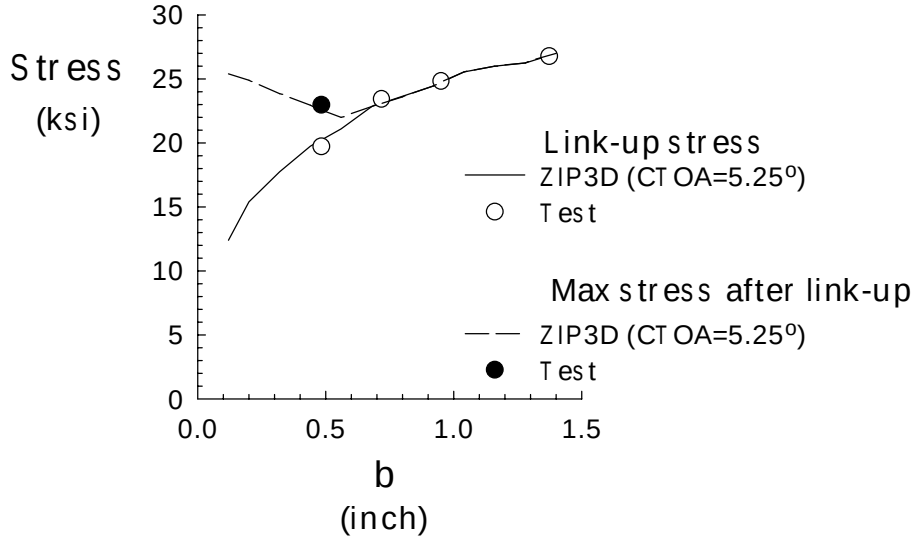

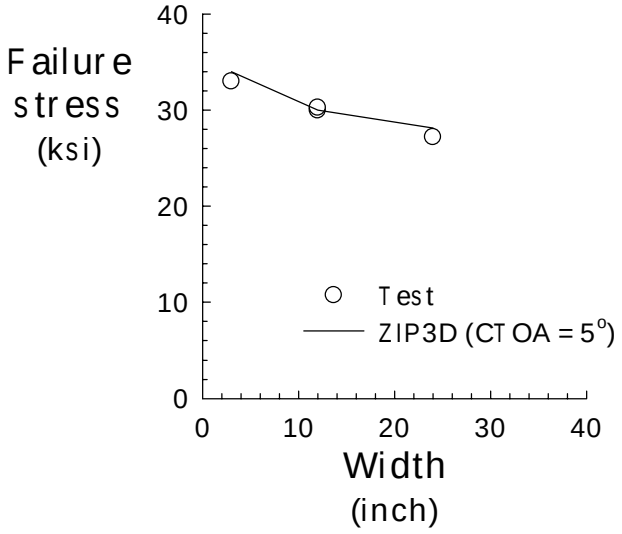

Figure 12 Experimental measurements and the ZIP3D finite element predictions for fracture tests conducted on 12-inch-wide, 2024-T3 aluminum alloy, 3-crack specimens.

Figure 13 Experimental measurements and the ZIP3D finite element predictions for fracture tests conducted on 0.063 inch thick 2024-T3 aluminum alloy in the T-L orientation.

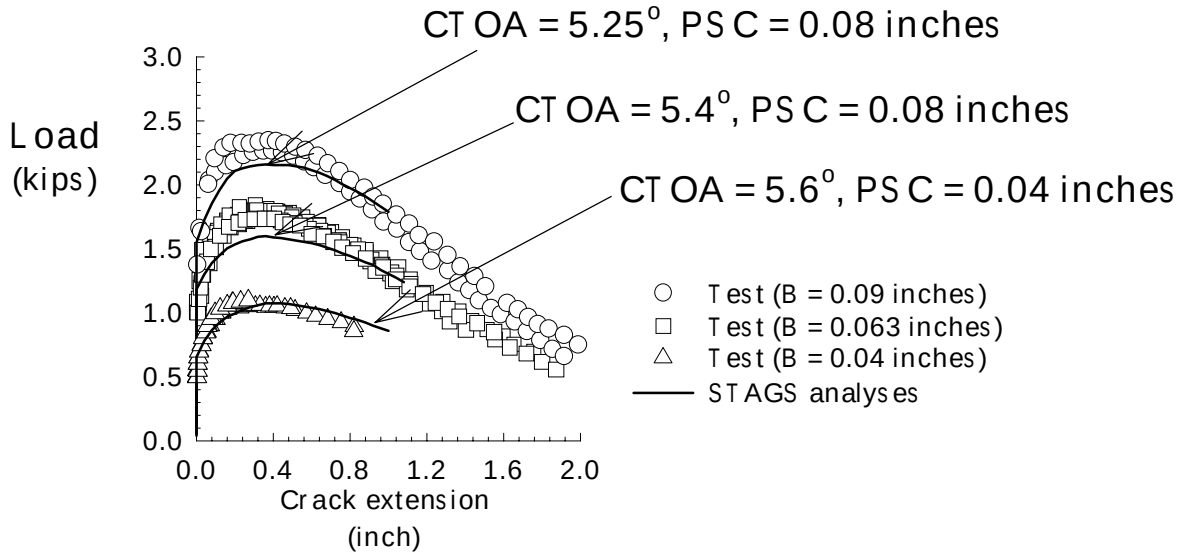

Figure 14 Fracture results from 6-inch-wide C(T) specimens with an initial crack length of a/W = 0.4 and the CTOA simulations using STAGS and the plane strain core approximation.

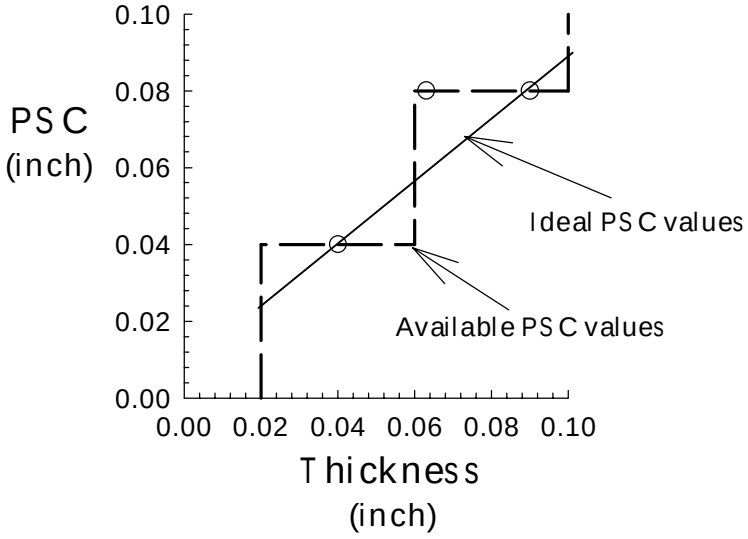

Figure 15 Plane strain core heights (PSC) for the 0.04, 0.063, and 0.09-inch-thick 2024-T3 aluminum alloy specimens.

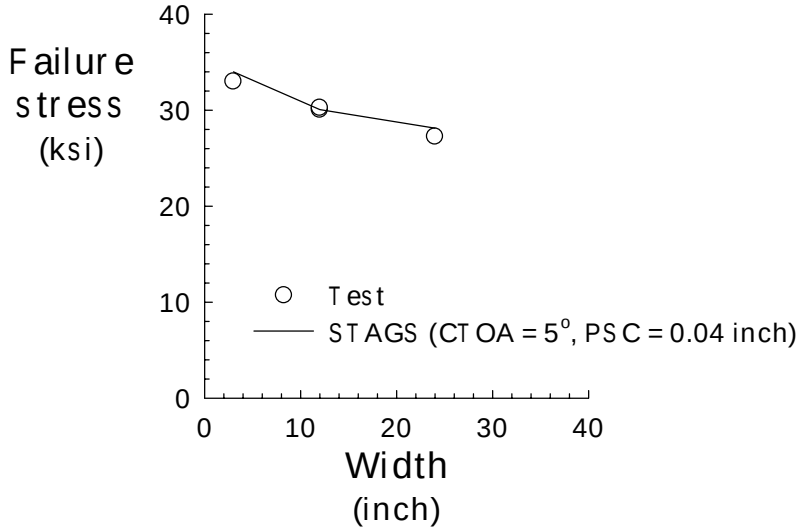

Figure 16 Experimental measurements and the STAGS finite element predictions (CTOA = 5^o and PSC = 0.04 inch) for the 0.063-inch-thick, 2024-T3 aluminum alloy M(T) specimens in the T-L orientation.

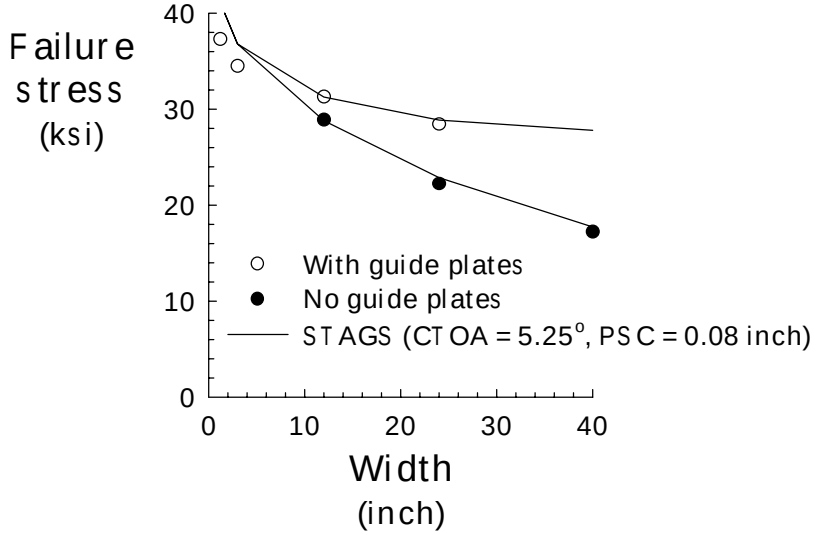

Figure 17 Fracture test results for 2024-T3, B = 0.09-inch-thick M(T) specimens (initial crack length 2a/W = 1/3) with and without guide plates and STAGS predictions using CTOA = 5.25^o and PSC = 0.08 inch.

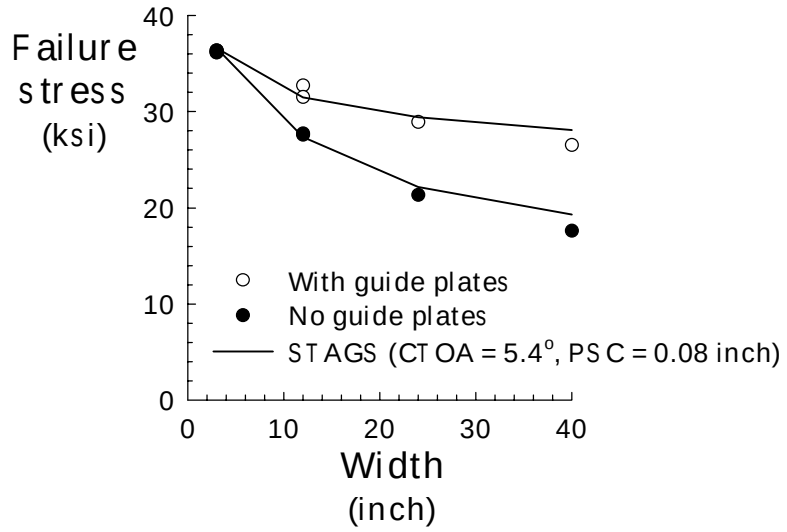

Figure 18 Fracture test results for 2024-T3, B = 0.063-inch-thick M(T) specimens (initial crack length 2a/W = 1/3) with and without guide plates and STAGS predictions using CTOA = 5.4° and PSC = 0.08 inch.

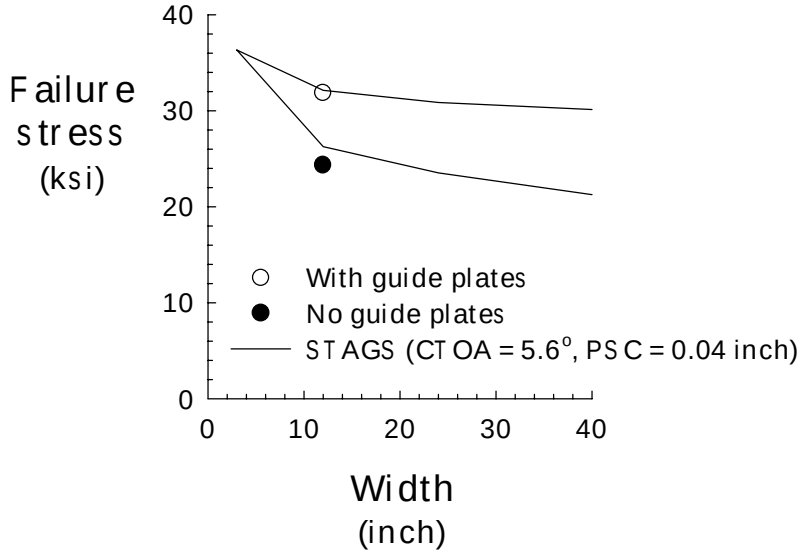

Figure 19 Fracture test results for 2024-T3, B = 0.04-inch-thick M(T) specimens (initial crack length 2a/W = 1/3) with and without guide plates and STAGS predictions using CTOA = 5.6° and PSC = 0.04 inch.

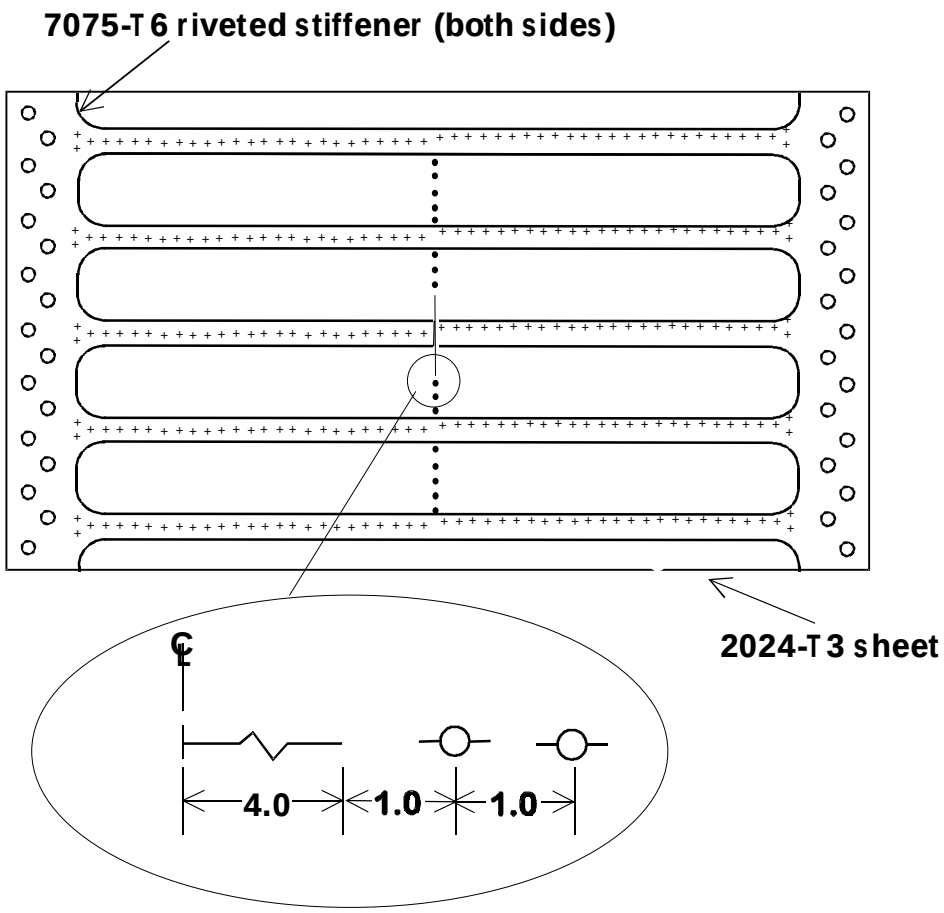

Figure 20. Stiffened panel and MSD crack configuration.

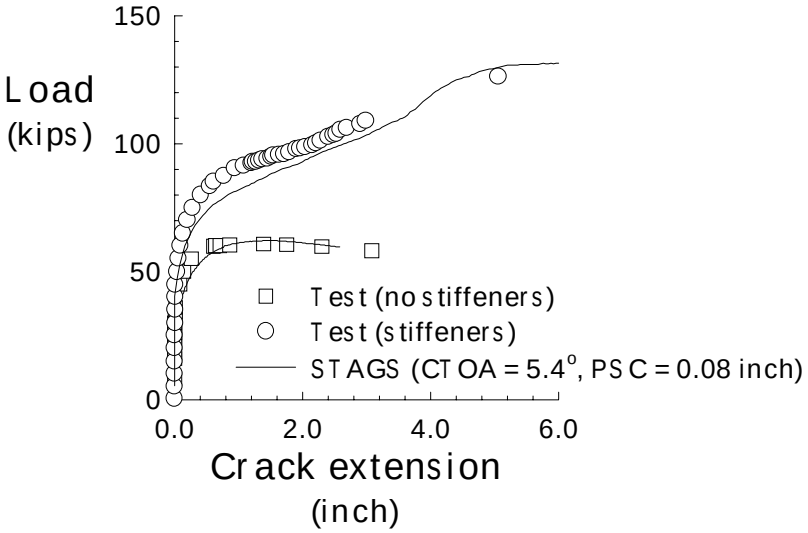

Figure 21. Fracture test results for 2024-T3, B = 0.063-inch-thick, 40-inch-wide M(T) specimens with and without stiffeners and STAGS predictions using CTOA = 5.4° and PSC = 0.08 inch.

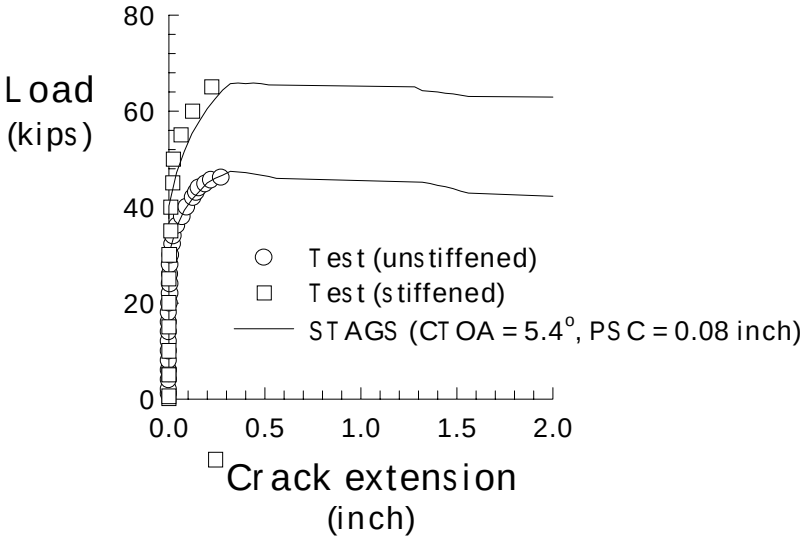

Figure 22 Fracture test results for 2024-T3, B = 0.063 inch thick, 40-inch-wide 0.05-inch-long MSD specimens with and without stiffeners and STAGS predictions using CTOA = 5.4° and PSC = 0.08 inch.

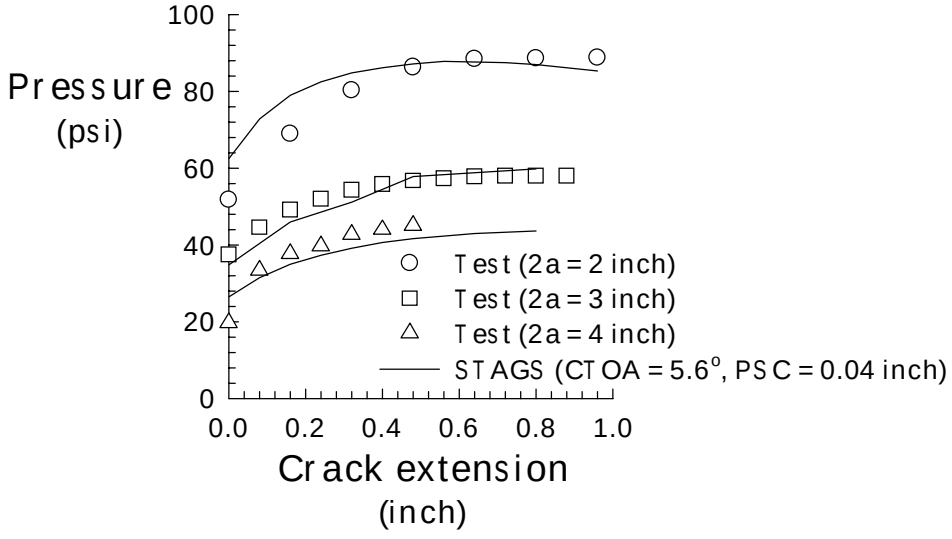

Figure 23 Experimental measurements and STAGS analyses (CTOA = 5.6° and PSC = 0.04 inch) for the 18-inch-diameter, 0.04-inch-thick 2024-T3 aluminum alloy pressurized cylinders.

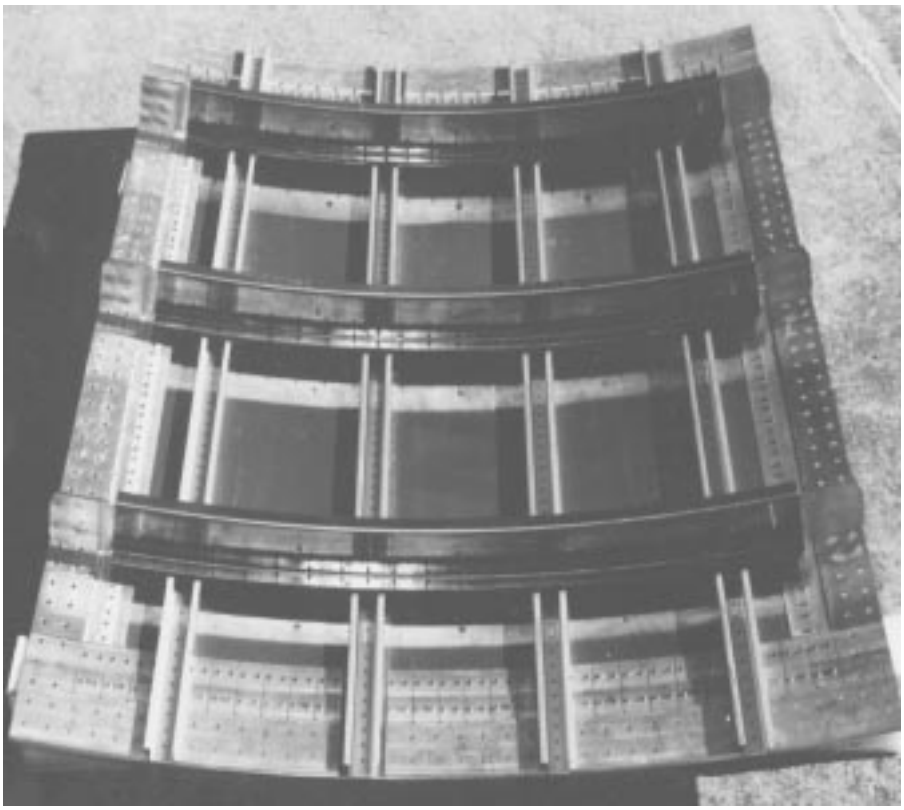

Figure 24a Photograph of the stiffened fuselage panel specimen.

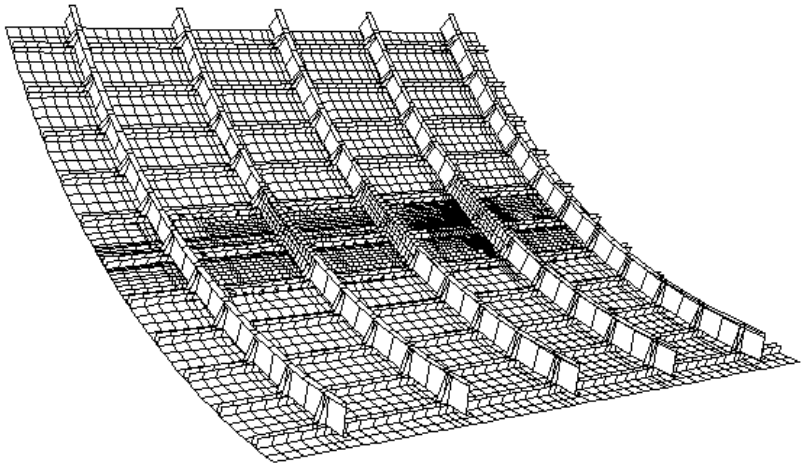

Figure 24b. Typical finite element mesh of a stiffened fuselage panel specimen.

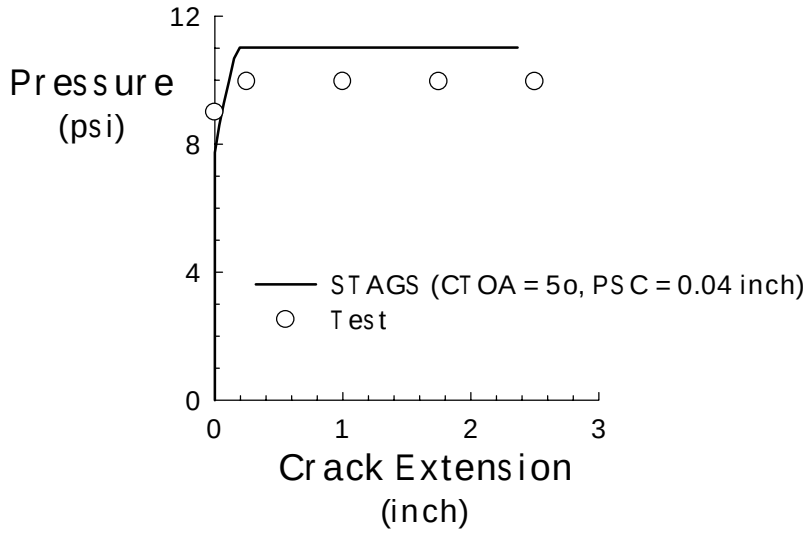

Figure 25. Experimental measurements and STAGS finite element predictions (CTOA = 5^{o} and PSC = 0.04 inch) for the pressurized fuselage test specimen.